Journal of Experimental Botany
https://doi.org/10.1093/jxb/eraf128 Advance Access Publication 19 March 2025

RESEARCH PAPER

Genomic and evolutionary evidence for drought adaptation of allopolyploid *Brachypodium hybridum*

Yuanyuan Wang[1,2], Guang Chen[3], Fanrong Zeng[4], Fenglin Deng[4], Zujun Yang[5], Zhigang Han[6], Shengchun Xu[3], Eviatar Nevo[7], Pilar Catalán[8,*], and Zhong-Hua Chen[2,*]

[1] College of Agriculture and Biotechnology, Zhejiang University, Hangzhou 310058, China
[2] School of Science, Western Sydney University, Penrith, NSW 2751, Australia
[3] Xianghu Laboratory, Hangzhou 310021, China
[4] Hubei Collaborative Innovation Center for Grain Industry, College of Agriculture, Yangtze University, Jingzhou 434025, China
[5] School of Life Science and Technology, University of Electronic Science and Technology of China, Chengdu, Sichuan 611731, China
[6] State Key Laboratory of Subtropical Silviculture, Zhejiang A&F University, Lin'an, Hangzhou, 311300, PR China
[7] Institute of Evolution, University of Haifa, Mount Carmel, 34988384 Haifa, Israel
[8] Department of Agricultural and Environmental Sciences, High Polytechnic School of Huesca, University of Zaragoza, Huesca, Spain

* Correspondence: z.chen@westernsydney.edu.au or pcatalan@unizar.es

Received 6 October 2024; Editorial decision 11 March 2025; Accepted 13 March 2025

Editor: Jianhua Zhang, Hong Kong Baptist University

Abstract

Climate change is increasing the frequency and severity of drought worldwide, threatening the environmental resilience of cultivated grasses. However, the genetic diversity in many wild grasses could contribute to the development of climate-adapted varieties. Here, we elucidated the impact of polyploidy on drought responses using allotetraploid *Brachypodium hybridum* (*B. hybridum*) and its progenitor diploid species *Brachypodium stacei* (*B. stacei*). Our findings suggest that progenitor species' genomic legacies resulting from hybridization and whole-genome duplications conferred greater ecological adaptive advantages to *B. hybridum* compared with *B. stacei*. Genes related to stomatal regulation and the immune response from S-subgenomes were under positive selection during speciation, underscoring their evolutionary importance in adapting to environmental stresses. Biased expression in polyploid subgenomes (*B. stacei*-type and *B. distachyon*-type) significantly influenced differential gene expression, with the dominant subgenome exhibiting more differential expression. *B. hybridum* adapted a drought escape strategy characterized by higher photosynthetic capacity and lower intrinsic water-use efficiency than *B. stacei*, driven by a highly correlated coexpression network involving genes in the circadian rhythm pathway. In summary, our study shows the influence of polyploidy on ecological and environmental adaptation and resilience in model *Brachypodium* grasses. These insights hold promise for informing the breeding of climate-resilient cereal crops and pasture grasses.

Keywords: *Brachypodium hybridum*, *Brachypodium stacei*, drought response strategy, genomics, polyploidy, stomatal regulation, transcriptomics.

Introduction

The global food-production system needs to adapt to increasingly common events of abiotic stresses such as drought, heat, salinity, and heavy metals (Lesk *et al.*, 2016; Adem *et al.*, 2020; Bai *et al.*, 2020; N-H. Wang *et al.*, 2023). The majority of human calories are ultimately derived from grass species, including staple cereal crops and food-producing animals fed on cereal grains and pasture grass (Godfray *et al.*, 2010, 2011). Therefore, global food security will benefit from a better understanding of the abiotic stress resilience of grasses (Brkljacic *et al.*, 2011). Since the 1990s, *Brachypodium distachyon* (*B. distachyon*) has emerged as an ideal grass model (Draper *et al.*, 2001; The International Brachypodium Initiative, 2010; Brkljacic *et al.*, 2011; Decena *et al.*, 2021; Hasterok *et al.*, 2022; Minadakis *et al.*, 2024), and its evolutionary relationship within the genus *Brachypodium* and with other grasses has been extensively studied (Catalán *et al.*, 2016; Diaz-Perez *et al.*, 2018; Gordon *et al.*, 2020; Sancho et al., 2022). Recently, the polyploid *Brachypodium hybridum (B. hybridum)* and its two diploid progenitor species, *B. distachyon* and *Brachypodium stacei* (*B. stacei*) were selected as a model complex to investigate the multiple origins and the adaptive consequences of allopolyploidy (Gordon *et al.*, 2020; Scarlett *et al.*, 2022; Mu *et al.*, 2023a, b; Campos *et al.*, 2024).

The annual *B. hybridum* is an allotetraploid (2n=4x=30; x=5+10) derived from the cross of *B. distachyon* (2n=2x=10; x=5) and *B. stacei* (2n=2x=20; x=10) diploid progenitor species followed by subsequent whole-genome duplications (WGDs) (Catalán *et al.*, 2012). Molecular evolutionary analysis indicated that *B. stacei* is the oldest diploid lineage within the genus *Brachypodium*, splitting from the common ancestor ~10 million years ago (Mya), followed by the divergence of the *B. distachyon* lineage at ~7 Mya (Catalán *et al.*, 2012; Sancho *et al.*, 2018, 2022). In nature, plant diversity and speciation are often facilitated by recurrent interspecific hybridizations and allopolyploidizations (Ramsey, 1998), and *B. hybridum* formed at least three times from reciprocal crosses (Mu *et al.*, 2023a). It was revealed that one D-plastotype (plastome derived from *B. distachyon*) and two S-plastotypes (plastome derived from *B. stacei*) lines were independently formed ~1.4 Mya, and ~0.14 Mya and ~0.13 Mya, respectively (Gordon *et al.*, 2020; Mu *et al.*, 2023a). Environmental niche modeling studies have shown that *B. distachyon*, *B. stacei*, and *B. hybridum* occupy overlapping but distinct ecological niches in their native circum-Mediterranean regions, with each species exhibiting different ranges of variation across environmental parameters (López-Alvarez *et al.*, 2015). Specifically, the environmental data indicate that *B. distachyon* grows in cooler, wetter, and higher-altitude areas compared with *B. stacei*, which thrives in warmer, drier, and lower-altitude environments. In contrast, *B. hybridum* occupies areas with intermediate conditions but also extends into low-altitude, warmer, and drier zones, similar to its *B. stacei* progenitor. These findings support the notion that the three species exhibit distinct ecological adaptations to their respective environments (López-Álvarez *et al.*, 2017). This evolutionary framework of ancestral and young allopolyploid plants provides unique opportunities for *Brachypodium* species to serve as bridges to accelerate the process of gene discovery for tolerance to abiotic and biotic stresses in cereal crops (Brutnell *et al.*, 2015).

The relationship between polyploidy and stress tolerance is well documented, particularly in the establishment and development of polyploid species. Polyploidy drives the evolution of chromosome numbers, genome size, repetitive DNA, genes, novel traits, and species diversification. With changing climates and new stresses, polyploid formation may increase in natural, managed, and disturbed environments (Heslop-Harrison *et al.*, 2023). Polyploid plants typically exhibit enhanced stress tolerance, which can be attributed to the increased genetic diversity and genomic complexity resulting from hybridization and WGDs (Soltis *et al.*, 2014; Van de Peer *et al.*, 2017; Doyle and Coate, 2019). Gene duplication triggered by polyploidy plays a crucial role in crop domestication and the breeding of stress-resistant varieties (Renny-Byfield and Wendel, 2014). Ancient WGDs have occurred throughout the evolution of eukaryotes, and a large proportion of major crop plants, such as bread wheat, cotton, maize, and soybean, are polyploids (Masterson, 1994). Notably, these ancient WGDs often coincide with periods of dramatic global change (Fawcett *et al.*, 2009; Landis *et al.*, 2018; Van de Peer *et al.*, 2020; Carruthers *et al.*, 2024) and particularly adaptation to extreme environments (van Laere *et al.*, 2011; Deng *et al.*, 2012; Manzaneda *et al.*, 2012; Bromham *et al.*, 2020; Cai *et al.*, 2021; Caperta *et al.*, 2020; Zhang *et al.*, 2020). WGDs may have facilitated the adaptation of plants to new conditions and thus their ability to survive ecological upheaval or even catastrophic events (Liu *et al.*, 2020; Ebadi *et al.*, 2023). For example, autotetraploid *Arabidopsis thaliana* (Chao *et al.*, 2013; Mattingly and Hovick, 2023), rice (*Oryza sativa*) (P.M. Yang et al., 2014), and watermelon (*Citrullus lanatus*) (Zhu *et al.*, 2018) tend to occupy drier habitats compared with their closely related diploids. The allotetraploidy in citrange (*Citrus sinensis* × *Poncirus trifoliata*) (Ruiz *et al.*, 2016; Mahmoud *et al.*, 2023) and wheat (*Triticum. aestivum* L., AABBDD) (Yang *et al.*, 2014a; Ma *et al.*, 2023) promote salt and drought tolerance. Understanding the role of polyploidy in the adaptation of *Brachypodium* to environmental challenges could provide important insights into plant breeding to produce climate-adapted cereal crops. However, the mechanistic basis of intraspecific and intra(sub)genomic variation of *Brachypodium*, especially the relationship between drought tolerance and ploidy segregation, is still elusive.

Opposite slopes at Mount Carmel, Israel, designated as 'Evolution Canyon' (EC), display large microclimatic contrasts between the hotter and drier tropical African south-facing slope and the temperate European north-facing slope (Nevo, 1995; Li *et al.*, 2016; Yablonovitch *et al.*, 2017; Kang *et al.*, 2019; H. Wang et al., 2020). The EC model reveals evolution at a

microscale involving biodiversity divergence, adaptation, and incipient sympatric speciation across life, from viruses and bacteria to fungi, plants, and animals (Nevo, 2012). In our previous study, we used wild barley, wild emmer wheat, *B. stacei*, and *B. hybridum* from EC to investigate the role of diploid and polyploid differentiation in the adaptation of grasses to drought (Y. Wang *et al.*, 2023). The current study aims to elucidate the role of polyploidy in drought-response strategies by comparing the physiological traits, genomic variation, and homeolog expression bias (HEB) between the *B. stacei* genome and the two subgenomes of *B. hybridum* (Bhs and Bhd).

Materials and methods

Plant materials and growth conditions

Accessions were collected from Lower Nahal Oren, Mount Carmel, Israel, at the EC African slope (AS) and European slope (ES). Plant growth conditions followed those described in Chen *et al.* (2019). Plants were cultivated in the same soil and fertilizer conditions at 22±2 °C (day) and 20±2 °C (night) and 60% relative humidity under a 14 h light/10 h dark photoperiod in a growth chamber. The drought treatments were induced 3 weeks after germination and monitored by using PR2 multi-depth soil moisture probes (Dynamax, USA). Gas exchange measurements and stomatal assays were performed and processed when the water-holding capacity was gradually maintained at 10% (v/v) in drought-treated plants. Leaf samples from well-watered and drought-treated plants were collected for RNA sequencing (RNA-seq) at the same time. At least three biological replicates were used for each sample and treatment.

Gas exchange measurement and stomatal assay

Net CO_2 assimilation, stomatal conductance, intercellular CO_2 concentration, transpiration rate, leaf vapor pressure deficit, and leaf temperature were measured with a LI-6400 infrared gas analyzer (Li-Cor Inc., Lincoln, NE, USA) (Liu *et al.*, 2017; Chen *et al.*, 2019). The measured parameters were set at: flow rate 500 mol s^{-1}, saturating photosynthetically active radiation 1500 μmol m^{-2} s^{-1}, 400 mmol mol^{-1} CO_2, relative humidity 60%. The ratio between net CO_2 assimilation rate and stomatal conductance was calculated as intrinsic water-use efficiency (WUE_i).

The stomatal assay was performed on abaxial epidermises; measurements were carried out as described previously (Liu *et al.*, 2017; Chen *et al.*, 2019). The stomatal assay was conducted from 10.00 h to 16.00 h in parallel with the gas exchange measurement. Abaxial epidermises were peeled and immersed in measuring solution (10 mM KCl, 5 mM Ca^{2+}-MES, pH 6.1) and mounted on slides. For each sample, at least 30 images were taken from at least five epidermis strips using a microscope with a CCD camera (Nikon, Tokyo, Japan). Stomatal parameters including aperture length and width, guard cell length and width, and subsidiary cell length and width were measured by ImageJ software (NIH, USA).

Genome evolution analysis

The command line program 'wgd' and related tools including BLASTP, MCL, PAML4, MAFFT, FastTree, and I-ADHoRe were used for WGD analysis (Zwaenepoel and Van De Peer, 2019). Coding sequence (CDS) files used in WGD analysis from three species of the complex were downloaded from Phytozome (https://phytozome-next.jgi.doe.gov/info/Bstacei_v1_1; https://phytozome-next.jgi.doe.gov/info/Bhybridum_v1_1; https://phytozome-next.jgi.doe.gov/info/Bdistachyon_v3_1); 'codeml' of PAML was used for calculating the Ka/Ks ratio [the number of non-synonymous substitutions per non-synonymous site (Ka)/the number of synonymous substitutions per synonymous site (Ks)]. Syntenic homeologs were identified for each pairwise species comparison with the MCScanX algorithm (Wang *et al.*, 2012) using default parameters with top five hits of each query of all-to-all BLASTP. Long terminal repeat retrotransposons (LTR-RTs) were identified using the LTR retriever (version 2.8) (Ou and Jiang, 2018).

RNA sequencing and data analysis

The RNA library preparation and the alignment for sequencing reads were conducted in a previous study (Y. Wang *et al.*, 2023). The dominant subgenome identification was based on *B. hybridum* homeolog gene expression characterized through the syntenic blocks. DESeq2 (Love *et al.*, 2014) was used to assess biased expression patterns of Bhs versus Bhd homeologs. For the well-watered control (C) and drought treatment (T) conditions, each pair of homeologs was split into two groups; homeologs in Bhs were set as the reference group. For a given gene, if the expression of the Bhd homeolog was significantly higher than that of the Bhs homeolog, it was designated 'Bhd-dominant', and the converse was designated 'Bhs-dominant'; homeologs showing equal expression were categorized as 'not biased'. The comparison of gene numbers showing biased and unbiased homeolog expression within or among the genotypes was visualized using UpSetR (1.4.0).

Weighted correlation network analysis (WGCNA) (Langfelder *et al.*, 2008) was used to find clusters and modules of highly correlated coexpressed genes of *B. hybridum* and *B. stacei*. Gene Ontology (GO) and Kyoto Encyclopedia of Genes and Genomes (KEGG) enrichment were created using clusterProfiler (4.14.6). The genic compositions of *B. hybridum* and *B. stacei* were determined with BLASTP, using as a reference the gene annotation database of *A. thaliana* (https://bioconductor.org/packages/release/data/annotation/html/org.At.tair.db.html). Initial components of protein-to-protein interaction networks were retrieved from the identified hub genes of the Mitogen-Activated Protein Kinase (MAPK)/circadian rhythm KEGG pathway. Public annotation data from Cytoscape (Su *et al.*, 2014) were used to construct the interaction network. In order to use familiar gene names instead of the automatically generated ones, the network node and edge files were first exported and then converted from ENTREZID to *A. thaliana* SYMBOL using clusterProfiler. The updated node and edge files were subsequently reimported into the software, and then the value of differentially expressed genes (DEGs) was used as the grouping information for color labeling.

Genome resequencing and data analysis

The whole-genome resequencing and single-nucleotide polymorphisms (SNPs) were derived from our previous study (Y. Wang *et al.*, 2023). The SNPs that excludes sites of 0.1 missing rate and minQ value >30 and minor allele frequencies (MAFs) <0.05 and minimum mean depth value >8 were regarded as high-quality SNPs. High-impact SNPs were annotated by SnpEff (LGPLv3). SNPGenie (v1.0) (Nelson *et al.*, 2015) was used to estimate non-synonymous diversity per non-synonymous site (πN)/synonymous diversity per synonymous site (πS) ratios from SNPs for potential selection in *B. stacei* and *B. hybridum*.

Results

Polyploidy and genomic adaptation of *B. hybridum* and *B. stacei*

Previously, we identified 19 *Brachypodium* accessions from AS and ES using centromeric and telomeric-specific probes in fluorescence *in situ* hybridization analysis, of which *B.*

hybridum (Bh) individuals were mainly from the dry and highlight AS and *B. stacei* (Bs) individuals were mainly from the wet and shady ES (Y. Wang *et al.*, 2023). The more mesic progenitor species *B. distachyon* is not currently present in EC (Mu *et al.*, 2023a). The time of divergence of pairs of genomes and/or subgenomes can be estimated from the synonymous substitution rates (Ks) using the equation T (divergence time) = Ks/2λ, where $\lambda = 6.5 \times 10^{-9}$ (Lynch and Conery, 2000; He *et al.*, 2013; Takahagi *et al.*, 2018) is the absolute mean rate of substitutions per site per year inferred for the grass genes (Fig. 1A). The Circos plot of intergenomic collinearity showed highly conserved blocks of genomic synteny of *B. stacei* and Bhs (Fig. 1B, Supplementary Table S1). The *B. hybridum* genome consists of a substantial amount of long terminal repeats (LTRs) such as Copia and Gypsy in the centromeric regions of the Bhs and Bhd chromosomes (Fig. 1B; Supplementary Table S2). The Bhd subgenome has 31% more Gypsy than the Bhs subgenome per kilobase, while the Bhs subgenome has 25% more Gypsy and 32% more Copia than the Bs diploid genome.

To identify genes under positive selection (Ka/Ks >1) during the evolution of *B. hybridum*, we calculated the Ka/Ks ratio for ortho-homeologs between *B. hybridum* and its diploid progenitors, *B. stacei* and *B. distachyon* (Fig. 1B; Supplementary Figs S1, S2). GO functional enrichment analysis revealed that genes with a Ka/Ks ratio >1 between *B. hybridum* and *B. stacei* are significantly associated with stomatal movement, stomatal complex development, immune response, and transmembrane transport (Supplementary Fig. S1). In contrast, genes with a Ka/Ks ratio >1 between *B. hybridum* and *B. distachyon* are predominantly involved in DNA transcription, RNA biosynthesis, gene expression, RNA metabolism, and flower development (Supplementary Fig. S2). We also identified 80 pairs of ortho-homeologs under positive selection in *B. hybridum*, shared between both the *stacei*-type (Bhs) and *distachyon*-type (Bhd) subgenomes (Supplementary Table S3). These findings highlight the evolutionary significance of these genes in shaping key physiological and developmental processes, contributing to the adaptation of *B. hybridum* to environmental challenges. Then,

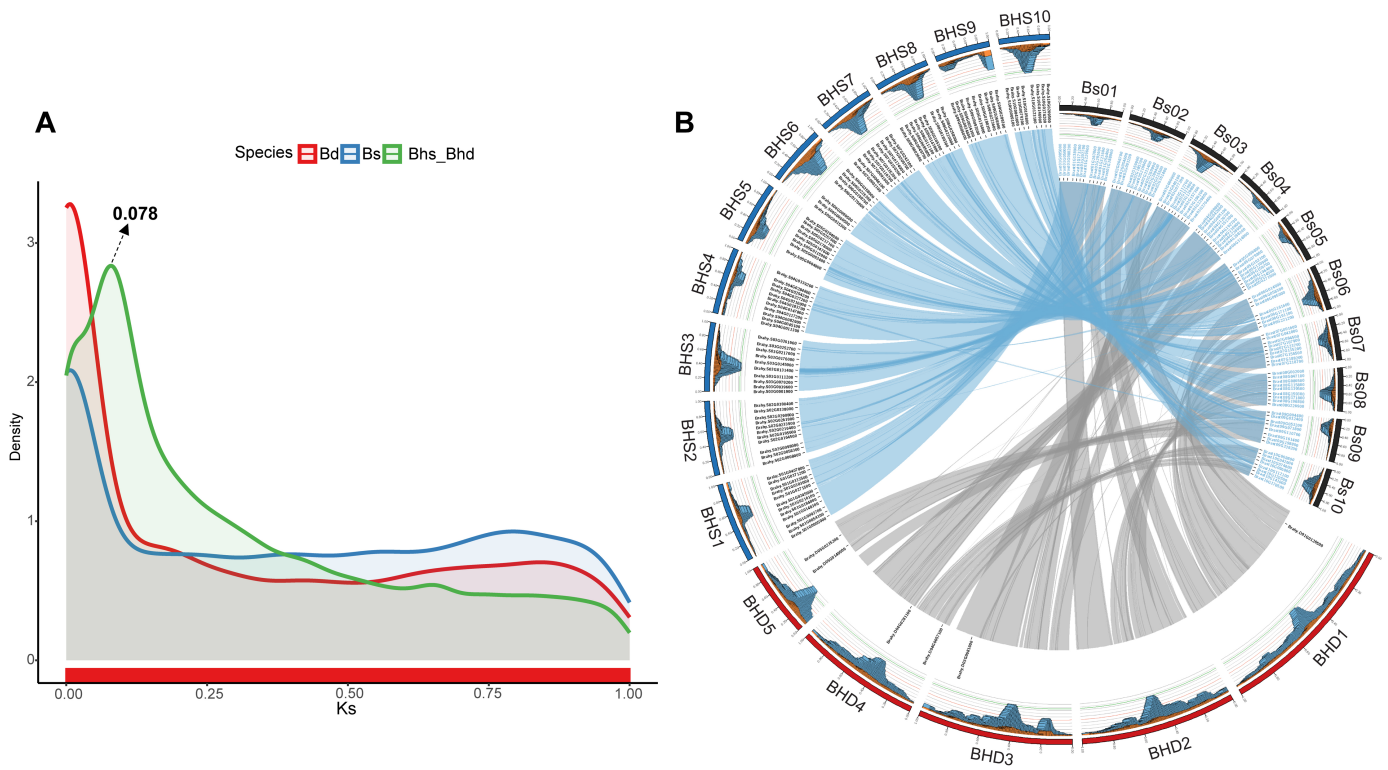

Fig. 1. Genomic evolution analysis of *Brachypodium* species. (A) Density of synonymous substitution rates (Ks) of *Brachypodium hybridum* (Bh), *Brachypodium stacei* (Bs), *Brachypodium distachyon* (Bd), Bhd versus Bs (Bhd_Bs), and Bhs versus Bd (Bhs_Bd). Ks values >1 were removed to eliminate saturated synonymous sites. The three peaks represent the divergence time between the subgenomes of the allotetraploid and each diploid genome and whole-genome duplication events of the allotetraploid. (B) Circos diagram depicting the genomic relationships of Bh and Bs. The chromosomes are shown along with their relative position. The outer track shows the distribution of long terminal repeat retrotransposons over each chromosome as stacked histograms; blue bars and orange bars represent Copia-domain distribution and Gypsy-domain distribution, respectively. The text in the inner ring demonstrates homeolog genes with the highest Ka/Ks values between the two species. The inner arcs designate intergenomic rearrangements.

we compared the stomatal traits of Bh and Bs (Fig. 2). Under well-watered conditions, Bh exhibited significantly larger stomatal aperture length (Fig. 2A, D), guard cell length and width (Fig. 2C, H, I), and subsidiary cell length (Fig. 2B, F) compared with Bs, which could be due to the polyploidy (higher number of gene copies) of Bh resulting in larger cell size. Bs displayed a larger aperture width (Fig. 2E) and subsidiary cell width (Fig. 2G). Drought led to a reduction in stomatal length and width in both *Brachypodium* species, with a more pronounced reduction in stomatal width in Bs (Fig. 2E, G). To further investigate the relationship between drought-induced changes in stomatal changes and transcriptional regulation, we examined the expression of key genes involved in stomatal development (Wang and Chen 2020). Our results revealed that drought caused differential expression of these stomatal regulation genes in both *B. hybridum* and *B. stacei* (Supplementary Table S4). Within each *Brachypodium* species, the response to drought was consistent across the genotypes. Additionally, the regulation of homologous genes in the S-subgenome of *B. hybridum* and *B. stacei* exhibited similar patterns between the species. These findings suggest that the identified stomatal regulation genes play a crucial role in the species' adaptive responses to drought and has remained conserved during the evolution of *B. hybridum*.

Transcriptional landscapes of the drought response in *B. hybridum* and *B. stacei*

Bh and Bs accessions showed distinct stomatal and photosynthetic responses to drought. Under drought treatment, Bh accessions maintained a significantly higher photosynthesis rate, stomatal conductance and stomatal aperture area, a lower WUE_i (Supplementary Fig. S3), and had an earlier flowering time than *B. stacei* (Y. Wang *et al.*, 2023). To reveal

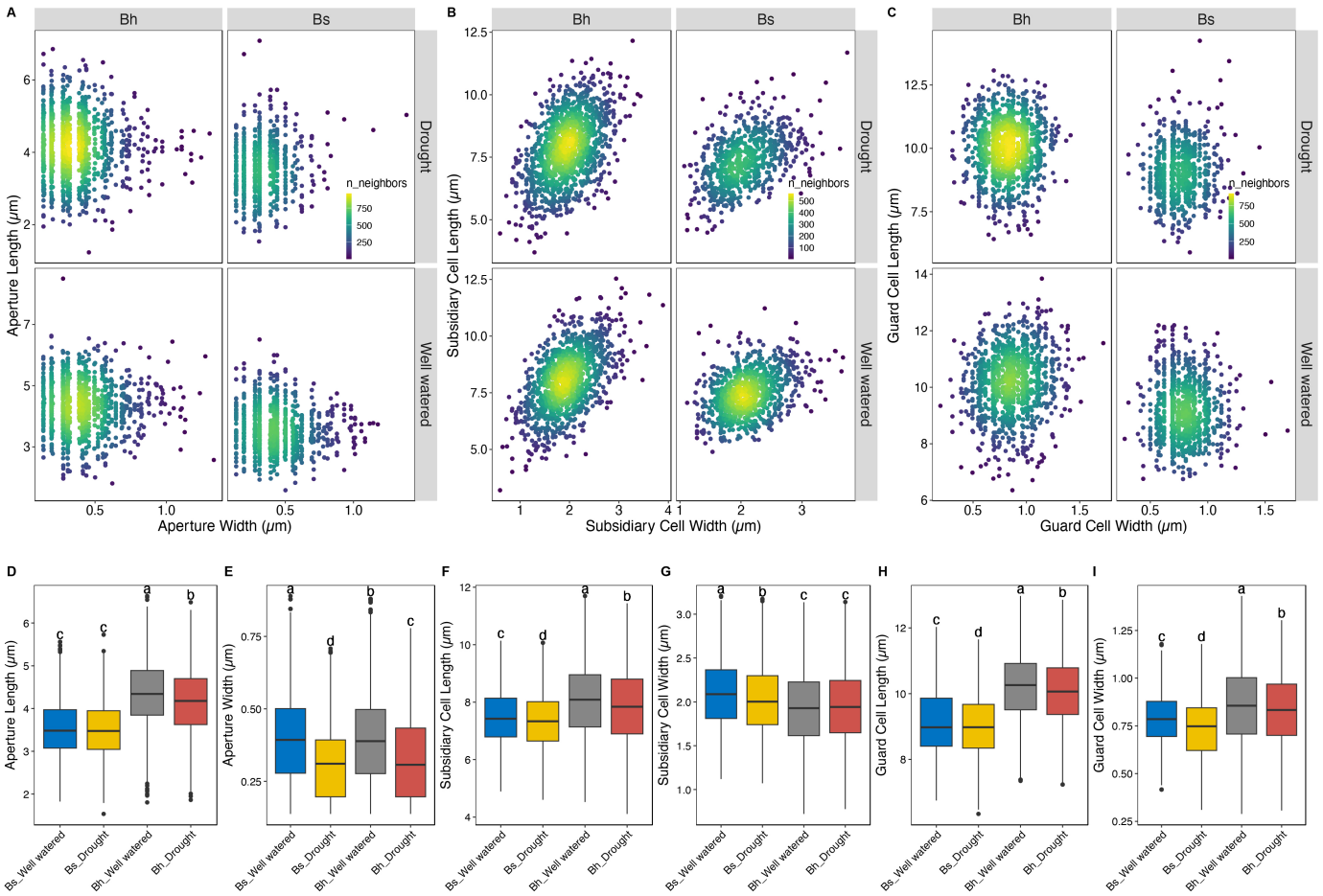

Fig. 2. Stomatal structure of *Brachypodium stacei* and *Brachypodium hybridum* in response to drought. (A) Stomatal aperture length and width, (B) subsidiary cell length and width, (C) guard cell length and width; (D–I) comparison of stomatal parameters between *B. stacei* and *B. hybridum.* In (A–C), the data are visualized using scatter density plots, where the color gradient represents the density of neighboring data points (n_neighbors), with yellow indicating higher density and purple indicating lower density. The upper panels show measurements made under drought conditions and the lower panels show measurements made under well-watered conditions. The results highlight differences in stomatal and subsidiary cell structure between the two species and the impact of drought on these parameters. In (D–I), differences between groups were determined using one-way ANOVA with a post-hoc Tukey HSD test. Significant differences ($P<0.05$) are indicated with different letters above the plots.

the molecular mechanisms underlying the physiological differences between Bh and Bs, we conducted RNA-seq of these *Brachypodium* accessions (Supplementary Table S5). The transcriptomic profiles of the subgenomes of Bs and Bh could be clearly separated by principal component analysis (Supplementary Fig. S4). We identified ortho-homeolog triads using the collinear results for a global comparison between the Bs genome and the Bhs and Bhd subgenomes of *B. hybridum*. Genes that were differentially expressed in >30% (i.e. >3) accessions of each *Brachypodium* species were identified as DEGs. A Venn plot showed that Bs shares more DEGs with Bhs than with Bhd (Fig. 3A). Shared DEGs in Bhs, Bhs, and Bs were primarily involved in responses to environmental stress, such as light intensity, starvation, nutrient level, and hypoxia, whereas unique DEGs in Bhs showed enrichment in circadian rhythm and rhythmic process, and those in Bs were associated with pollen recognition and defense responses (Fig. 3B).

We further assessed homeolog expression bias under well-watered and drought conditions to validate whether drought governs shifts in gene expression between Bhs and Bhd. Although most genes showed balanced expression, there were 2383 and 2228 pairs of ortho-homeologs dominated by Bhd or Bhs, respectively, under both the control and drought condition (Fig. 3C); these two sets of genes are enriched in different biological processes. Bhs genes are primarily enriched in functions related to environmental stimuli, such as defense response to bacteria and response to heat (Supplementary Fig. S5). In contrast, Bhs genes have more DEGs related to DNA damage stimulus, DNA repair, and regulation of the cell cycle (Supplementary Fig. S5). Approximately 500 genes are commonly dominated by both the S and D subgenomes across

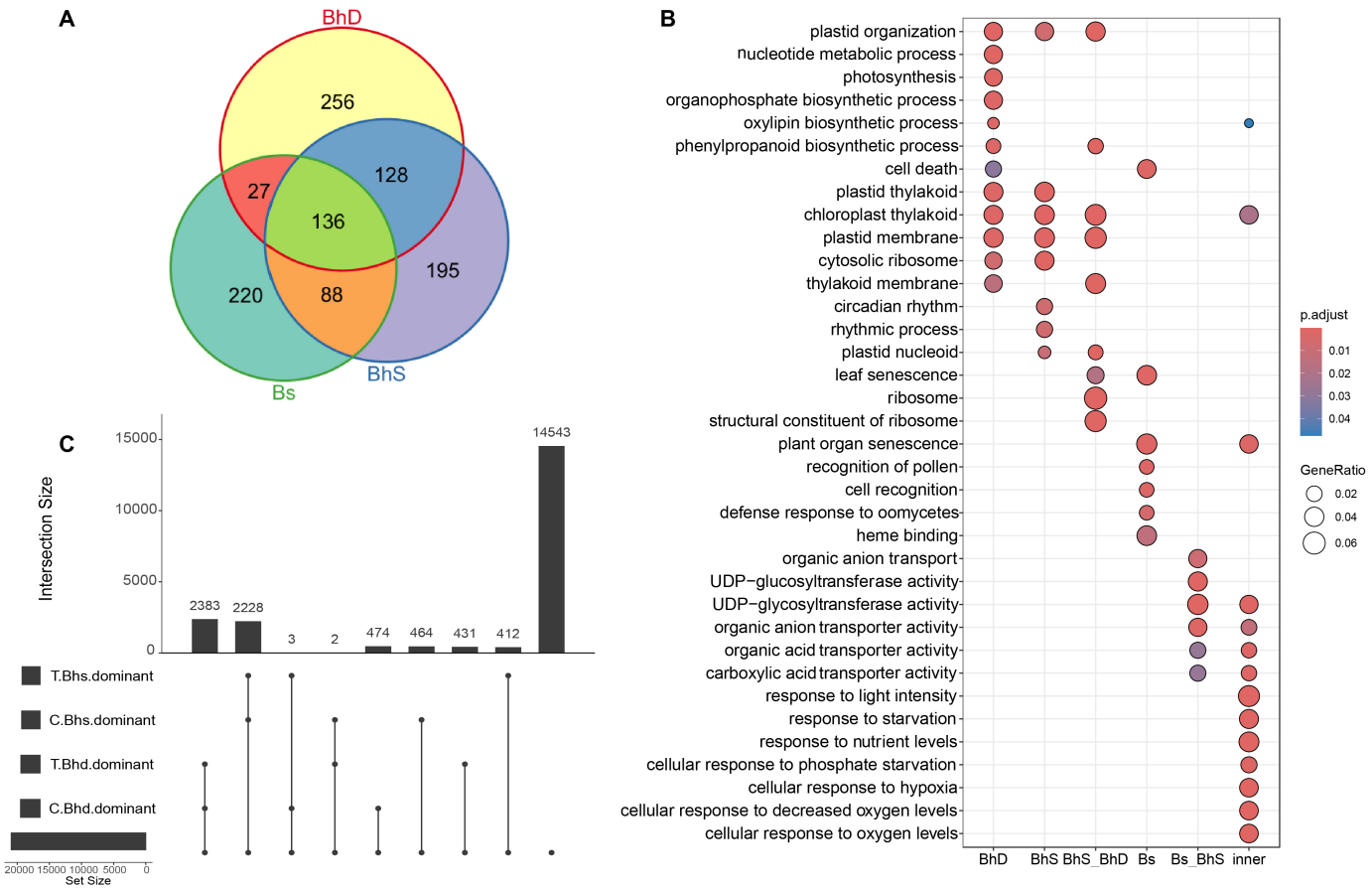

Fig. 3. Global transcriptome analyses of the drought response in *Brachypodium hybridum* and *Brachypodium stacei*. (A) Venn plot of differentially expressed genes (DEGs) in subgenomes of *B. hybridum* and in *B. stacei*; genes that are differentially expressed in more than 30% of the accessions within each species were considered DEGs. (B) Gene Ontology enrichment analysis for the intersections of DEGs in the Venn plot; 'inner' represents the 136 genes differentially expressed in Bhd, Bhs, and Bs. (C) Expression differentiation of paired homeolog genes between *B. hybridum* subgenomes. Homeolog gene pairs were identified by collinear blocks using the Bhs subgenome as the reference for each pair. The black horizontal bars on the left of the figure show the number of paired homeolog genes dominated by the Bhs/Bhd subgenome under well-watered (control; C) or drought (treatment; T) conditions. The lines with dots indicate genes sharing the same homeolog expression bias. The gene numbers of intersections are represented by the vertical bars.

all accessions, but the number of commonly dominated genes decreased to 178 and 162 for the S and D subgenomes, respectively, in response to drought (Supplementary Fig. S6). Moreover, five ortho-homeologs changed their dominant subgenome after drought treatment (Supplementary Table S6).

We compared the proportion of balanced versus unbalanced expression patterns in non-DEGs (Fig. 4A) and DEGs (Fig. 4B) across species/subgenomes. The results showed that 70% of non-DEGs exhibited balanced expression, whereas this proportion decreased to 42–49% among DEGs. Notably, among the DEGs in the Bhd subgenome, Bhd-dominant genes under both control and treatment conditions accounted for a higher proportion. Similarly, among the DEGs in the Bhs subgenome or their homologous genes in *B. stacei*, Bhs-dominant genes also constituted a greater proportion under both control and treatment conditions. (Fig. 4B). This observation indicates that biased expression in the subgenomes of polyploid Bh is significantly influenced by parental legacy, with the dominant subgenome Bhd being more prone to differential expression among the DEGs induced by drought.

We employed RNA-seq and physiological traits of each accession to conduct WGCNA. Overall, 24 and 20 coexpression gene modules were clustered in Bh and Bs, respectively. The correlations among physiological traits were similar in Bh and Bs (Fig. 5). Moreover, Bh showed more coexpression modules significantly correlated with the physiological traits. Notably, ortho-homeologs in Bh that are enriched in 'circadian rhythm', 'rhythmic process', and 'response to blue light' showed a positive correlation with net photosynthetic rate and stomatal conductance, but a negative correlation with WUE_i (Fig. 6). In the coexpression network, several highly connected hub genes were identified, many of which are enriched in the MAPK KEGG pathway (Supplementary Fig. S7). An important difference between Bh and Bs in MAPK signaling was the regulation of genes encoding the plasma membrane receptor kinase FLAGELLIN SENSING 2 (FLS2), which participates in pathogen attack-triggered stomatal closure (Spallek *et al.*, 2013). The expression of genes involved in the abscisic acid (ABA) signaling pathway (*OST1*, *open stomata 1*; *HAB*, *Hypersensitive to ABA*; *PYL5*, *pyrabactin resistance 1-like 5*; *HAI*, *highly ABA-induced PP2C gene 1*; *CBL-interacting protein kinase*) was very similar between Bh and Bs. This thus indicates that although drought primarily affected the ABA signaling pathway, it also regulated other networks particularly involved in key hubs such as MAPK (Supplementary Figs S8, S9).

Genomic variants and positive selections in *B. hybridum* and *B. stacei*

To identify potential adaptive alleles in response to the drought environment in the AS, the genomes of all 19 accessions of

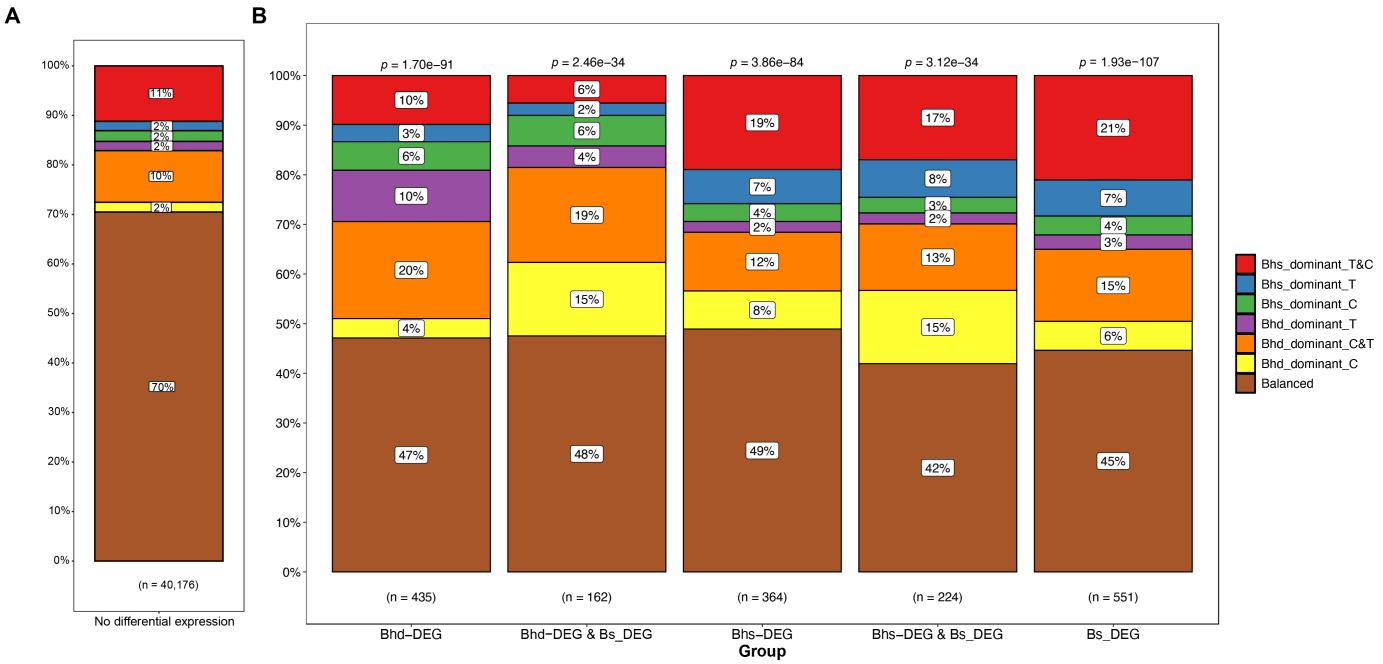

Fig. 4. Proportion of non-differentially expressed genes (A) and differentially expressed genes (DEGs) (B) balanced or predominantly expressed in each subgenome of *Brachypodium hybridum* and their homologous genes in *Brachypodium stacei*. Different colors distinguish the subgenomes that dominate gene expression under control (well-watered) or treatment (drought) conditions. Each bar represents a specific category of DEGs, with 'n' showing the number of genes in each category. Bhd-DEG and Bhs-DEG refer to DEGs specific to the Bhs or Bhd subgenome, respectively; Bhd-DEG & Bs_DEG and Bhs-DEG & Bs_DEG represent DEGs shared between the Bhd/Bhs subgenome and their corresponding homologous genes in *B. stacei*, respectively. The *P*-values above each bar denote the statistical significance among different expression patterns in each category.

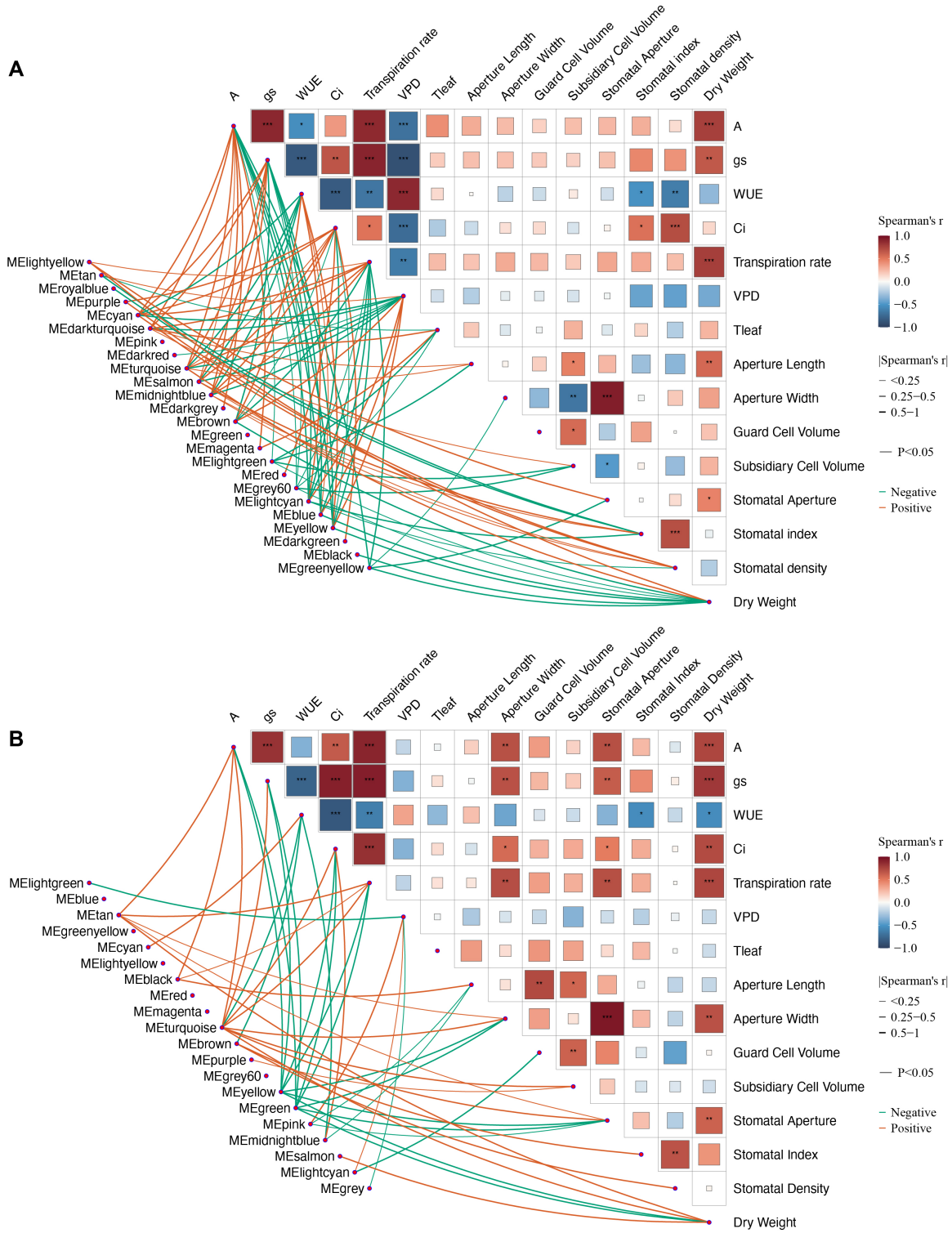

Fig. 5. Significant associations between gene clusters and physiological traits in (A) *Brachypodium hybridum* and (B) *Brachypodium stacei.* A triangular correlation plot was created to display the relationships between physiological and stomatal parameters. Red indicates positive correlations, blue represents negative correlations, and asterisks denote the significance of the correlations (*P<0.05, **P<0.01, ***P<0.001). The lines connected to each parameter represent coexpressed gene modules, with only those showing significant correlations retained. Red lines indicate positive correlations, green lines indicate negative correlations, and the thickness of the lines represents the Spearman's r value. A, net CO_2 assimilation; Ci, intercellular CO_2 concentration; gs, stomatal conductance; Tleaf, leaf temperature; VPD, vapor pressure deficit; WUE, water use efficiency.

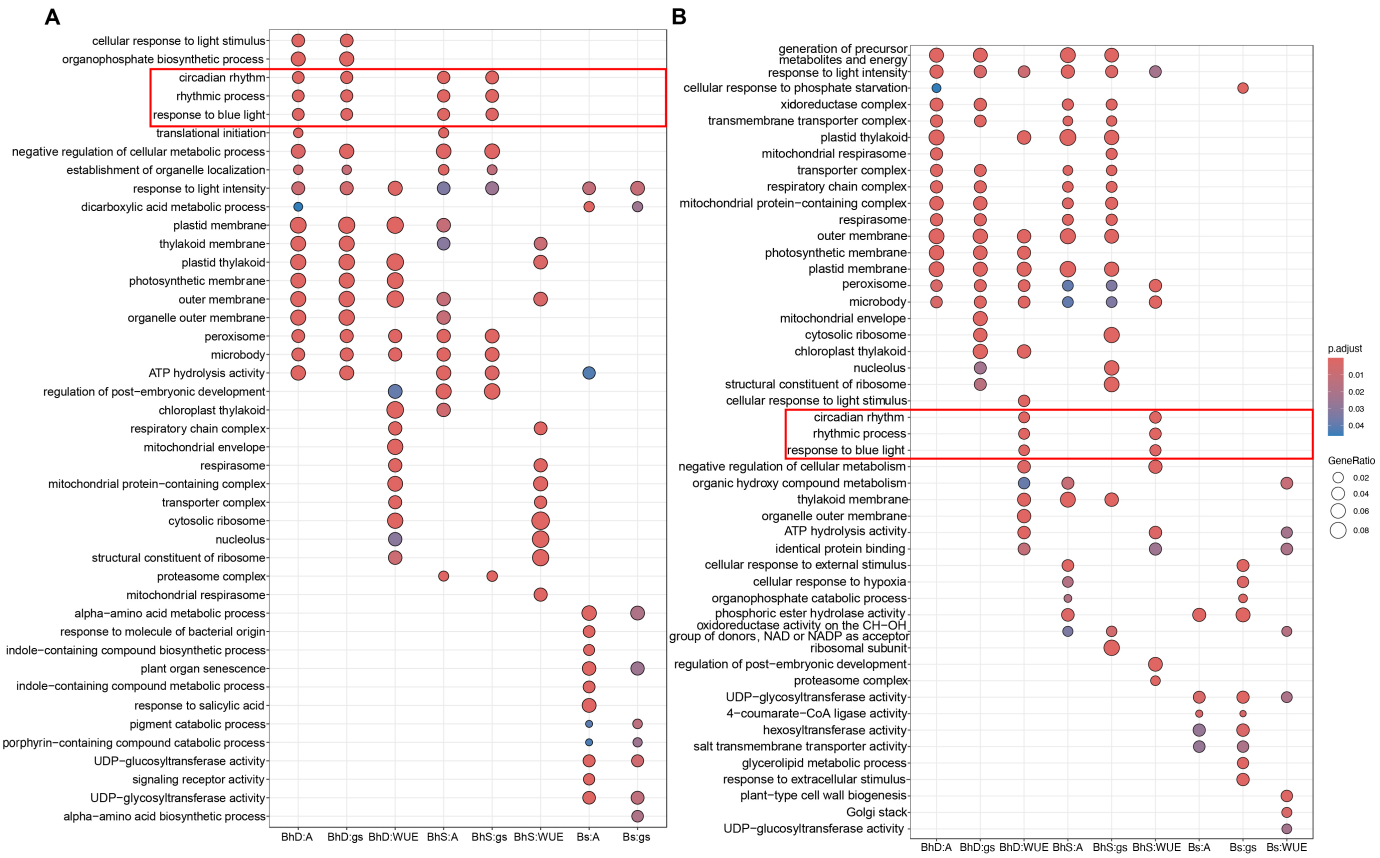

Fig. 6. Gene Ontology terms of gene modules significantly positively (A) and negatively (B) correlated with physiological traits across different subgenomes.

Bh and Bs were resequenced, yielding 794 Gb of clean data (Supplementary Table S5). After filtering, 1 142 287 and 614 074 high-confidence SNPs, along with 165 880 and 99 276 indels, were identified in Bh and Bs, respectively. These variants were distributed across 2090 genes in Bh and 669 genes in Bs (Fig. 7A). Among these, 363 and 140 genes in Bh and Bs, respectively, contained high-impact variants. Notably, some genes overlapped between Bh and Bs, particularly those with NB-ARC and P450 domains or those involved in plant biotic resistance such as plant–pathogen and plant–herbivore interactions (Supplementary Table S7). Based on πN and πS values calculated from SNPs, genes under positive selection ($\pi N/\pi S > 1$) in the two subgenomes of Bh were primarily associated with stomatal movement regulation and immune response. However, in Bs, they were linked to response to nitrate, immune response, biosynthetic processes, and calcium binding (Fig. 7B). Interestingly, these positively selected genes were also influenced by homeolog expression bias. For example, in Bhs, genes under positive selection showed a reduction in the proportion of Bhd-dominant homeologs, whereas in Bhd genes under positive selection exhibited a decreased proportion of Bhs-dominant homeologs (Fig. 7C). We identified DEGs in response to drought that were influenced by high-impact SNPs in *B. hybridum* and *B. stacei* (Supplementary Table S8), including some key genes involved in the ABA signaling pathway and plant innate immune responses, such as *PBL14* (*RPM1-induced protein kinase 14*), *AEP2* (*asparaginyl endopeptidase 2*), and *OSM34* (*osmotin 34*).

Discussion

Recent hybridization and whole-genome duplications provide drought adaptive potential for *B. hybridum*

Numerous studies have emphasized the impact of hybridization and WGD on gene expression patterns (Feldman *et al.*, 2012; Renny-Byfield and Wendel, 2014; Ramírez-González *et al.*, 2018) through the neofunctionalization of duplicated genes (Kondrashov, 2012) or tissue-specific expression of genes (Makova and Li, 2003). Polyploids, in general, can exhibit rapid adaptive responses under stress. For example, hexaploid wheat exhibits greater salt tolerance than its tetraploid and diploid ancestors, primarily due to the immediate transcriptional reprogramming of the D-subgenome *HKT1;5* homeolog, which is responsible for removal of Na^+ from the xylem. This gene shifts from high basal expression in the diploid parent

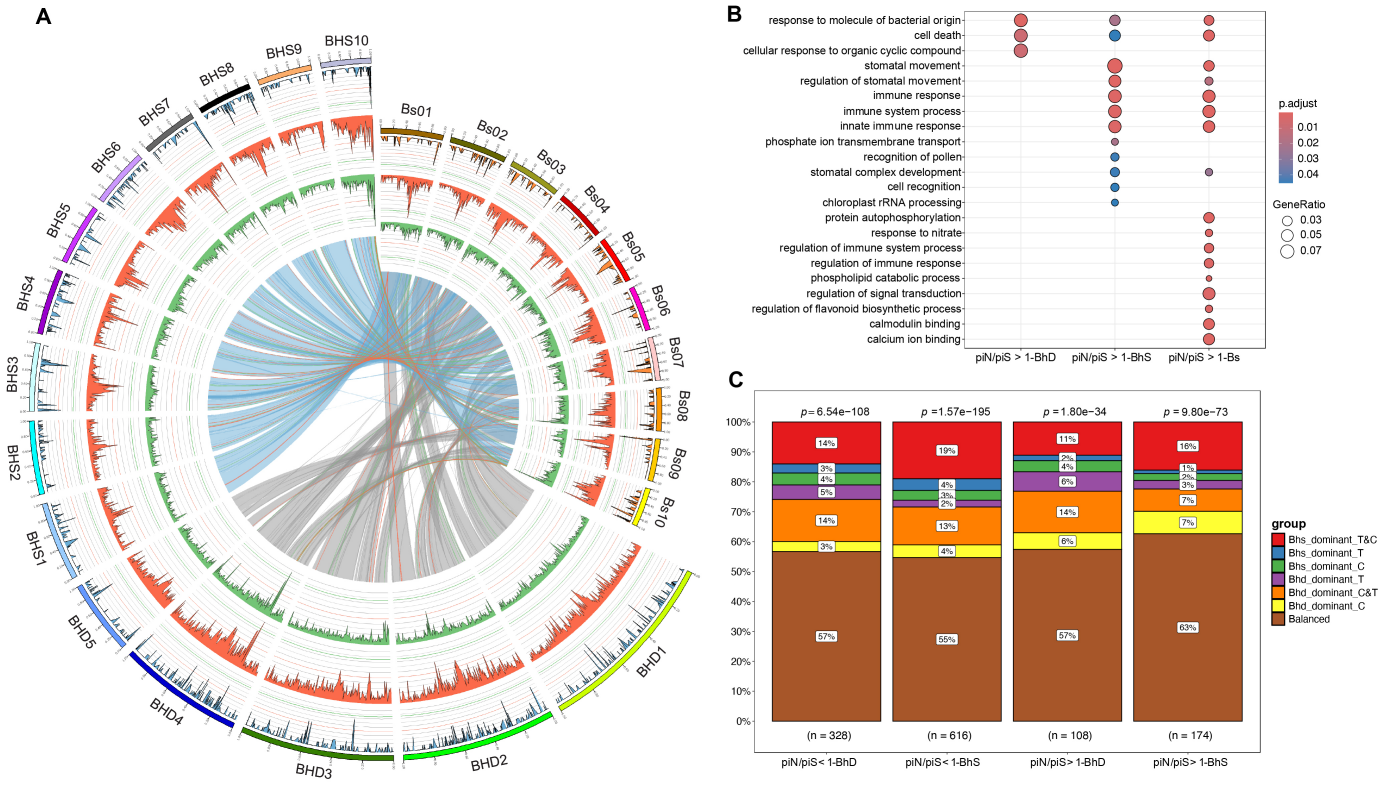

Fig. 7. Genome resequencing and the relationship between genes under selective pressure and expression patterns in *Brachypodium hybridum and Brachypodium stacei*. (A) Circos plot representing, from the outer to the inner circle, the number of variants with high impact (gain/lost stop_codon) of each gene of Bh (blue) and Bs (orange), single nucleotide polymorphism (SNP) density (red), and indel density (green). The inner arcs designate interchromosomal rearrangements; red and green lines represent enriched high-impact variants of Bh or Bs, respectively. (B) Gene Ontology terms for genes with high-impact SNPs. piN/piS indicates the ratio of non-synonymous to synonymous SNPs. (C) Proportion of genes under selective pressure with balanced or predominant expression in each subgenome of *B. hybridum*. Different colors distinguish the subgenomes that show dominant gene expression under control (well-watered) or treatment (drought) conditions. Each bar represents a specific category of genes, with 'n' showing the number of genes in each category. The *P*-values above each bar denote the statistical significance among different expression patterns in each category.

to salt-induced expression in the hexaploid, illustrating how subgenome-dominant functionalization contributes to the broad adaptability of hexaploid wheat under stress (C. Yang *et al.*, 2014). Similarly, Gui *et al.* (2021) compared four tetraploid and four hexaploid wheat species under drought stress, showing that hexaploid species exhibited significantly higher grain yield, harvest index, and water use efficiency (WUE) than tetraploid species. Dong *et al.* (2022) examined salt tolerance in four closely related diploid and polyploid cotton species, finding that allopolyploid species exhibited greater stress response flexibility compared with their diploid ancestors. By categorizing four distinct homeolog expression bias patterns, they highlighted the transcriptional effects of duplicated genes in polyploids under salt stress, shedding light on the adaptive role of allopolyploidization in stressful environments. In the present study, we observed that a subset of genes of *B. hybridum* was dominated by a single subgenome in both well-watered and drought conditions. This suggests that the transcriptional regulation of allotetraploid *B. hybridum* is shaped by subgenome-dominant expression patterns. Furthermore, the hypothesis that suggests that allopolyploid species utilize the expression patterns of both progenitor subgenomes depending on the environment (Shimizu-Inatsugi *et al.*, 2017) was validated in our analysis (Supplementary Table S6). Specifically, five ortho-homeologs exhibited changes in their dominant subgenome after drought treatment. For instance, one of the five genes, *AGAMOUS-like 66* (*AGL66*), is expressed in pollen to form heterodimers with other *MICK* (*MADS box, Keratin binding domain, and C terminal domain containing*) family members. It plays a key role in the late stages of pollen development and pollen tube growth (Adamczyk and Fernandez, 2009). Under drought conditions, the dominant expression of this gene shifts from the Bhd subgenome to the Bhs subgenome, which may contribute to the progenitor's ability to better adapt to drought conditions (Manzaneda *et al.*, 2012). Similarly, *Auxin-Induced in root cultures 3* (*AIR3*) acts downstream of *NAC1* to regulate lateral root development in Arabidopsis (Chen *et al.*, 2016). After drought stress, the dominant expression of *AIR3* shifts from the Bhs subgenome to the Bhd subgenome. This may reflect the observed differences in root system development between species under well-watered conditions, where *B. stacei* developed the largest root system and shoot dry weight, followed by

B. hybridum and *B. distachyon* (González *et al.*, 2020). The shift in gene expression after drought stress could be linked to the corresponding changes in root development, potentially contributing to drought tolerance.

The collinearity of genes in plant genomes generally decreases with increasing evolutionary distance (Wicker *et al.*, 2010). Here, we showed that the two subgenomes of *B. hybridum* share strongly conserved syntenic blocks with their corresponding progenitor diploids (*B. stacei*, Figs 1, 7; *B. distachyon*, Gordon *et al.*, 2020). It was reported that syntenic breakpoints are hotspots of evolutionary novelty that could act as a reservoir for producing adaptive phenotypes (Murat *et al.*, 2010). The deranged blocks may be disturbed by chromosomal recombination during interspecific hybridization. However, strong karyotypic differences between the Bs and Bd chromosomes probably prevented intersubgenomic chromosome rearrangements in *B. hybridum* (Mu *et al.*, 2023a). The evolutionary potential and high frequency of polyploidy or hybridization in flowering plants are also due to the activity of transposable elements, among which LTRs are abundant (Oliver *et al.*, 2013). They have a strong impact on the structure, function, evolution, and especially genome size of their host genome (Baidouri and Panaud, 2013). Here, the density distribution of Gypsy-type LTRs in Bh is obviously higher than in Bs because *B. hybridum* shows an additive pattern in LTRs; its LTR content is the result of the sum of LTRs from both progenitor species (Bhs and Bhd subgenomes) (Supplementary Fig. S10). However, the proportion with respect to the respective genome size is quite similar (Mu *et al.*, 2023a).

The crucial role of circadian rhythm regulation in the *B. hybridum* subgenome for its escape from drought

Exploration of divergent drought-tolerance strategies between tetraploids and their diploid progenitor species will provide new insights into the breeding of crops with improved adaptation to unpredictable environments. Under drought conditions, plants inevitably have a trade-off between carbon accumulation and the risk of deleterious soil water depletion; hence, plants have developed several strategies to cope with drought, including dehydration avoidance, drought tolerance, and drought escape (McKay *et al.*, 2003; Sherrard and Maherali, 2006; Tuberosa, 2012). The underlying mechanism of the drought-escape strategy employed by *B. hybridum* is likely to be regulated by light perception and the circadian clock to promote early flowering (Du *et al.*, 2018). In addition, early flowering can be achieved by maintaining rapid growth and high stomatal opening and photosynthesis rates, allowing the plant to complete its life cycle before the onset of severe water stress (Heschel and Riginos, 2005; Sherrard and Maherali, 2006; Donovan *et al.*, 2007; Wu *et al.*, 2010; Ivey and Carr, 2012; Manzaneda *et al.*, 2015).

Stomata play a crucial role in plant growth. Their function is constrained by a safety–efficiency trade-off, as plant survival depends on stomatal closure under drought conditions (Henry *et al.*, 2019). It has been shown that stomatal size is linked to WUE, which facilitates plant adaptive plasticity under drought stress (Dittberner *et al.*, 2018). One known function of polyploidy is the generation of larger cells (Frawley and Orr-Weaver, 2015), and polyploid plants typically have larger stomata than their diploid relatives, although they have fewer stomata per unit area. Similar observations have been made in species such as *Cannabis sativa* (Parsons *et al.*, 2019; Kurtz *et al.*, 2020), *Echinacea purpurea* (Abdoli *et al.*, 2013), and *Catharanthus roseus* (Xing *et al.*, 2011). In *Brachypodium* species, stomatal guard cell length has been identified as a useful trait to differentiate *B. distachyon* complex species from related diploid and polyploid grasses (Borrino and Powell, 1988; Katsiotis and Forsberg, 1995; Catalán *et al.*, 2012). We observed that *B. hybridum* accessions have larger stomata than *B. stacei* (Fig. 2), consistent with previous findings comparing the allotetraploid *B. hybridum* with its progenitor species *B. distachyon* (Catalán *et al.*, 2012; Manzaneda *et al.*, 2015). The specialized stomatal structures resulting from polyploidy in annual *Brachypodium* species may contribute to *B. hybridum*'s enhanced drought tolerance. Since increased stomatal size may alter WUE to affect reproductive success, the lower WUE associated with larger stomata in polyploids may be exacerbated by future atmospheric CO_2 concentrations (Šmarda *et al.*, 2023). It will be intriguing to explore whether polyploidy induces selective pressure on genes regulating cell size and cell-fate decisions in the future.

The internal timekeeper circadian clock of plants can anticipate environmental stimuli such as light and temperature to prepare for upcoming challenges. The plant circadian clock also participates in multiple pathways regulating functions such as photosynthesis, seed germination, stomatal movement, pollination, flowering, and senescence (Srivastava *et al.*, 2019). Therefore, we propose that the interconnection between ABA signaling and circadian rhythm regulation may explain why drought-escaping *B. hybridum* accessions maintain higher stomatal conductance and stomatal aperture area (Figs 5, 6), implying that the circadian clock provides optimal utilization of the plant machinery to achieve improved adaptation in response to abiotic stresses (Grundy *et al.*, 2015).

Linking drought-stress signalling with biotic resistance in *B. stacei*

Water deficit affects a large spectrum of plant functions, such as transpiration, photosynthesis, tissue growth, and reproductive development (Chaves *et al.*, 2003; Khalid *et al.*, 2023). Components of MAPK cascades are regarded as converging points of abiotic and biotic stress signaling (Xiong and Yang, 2003; Chinnusamy *et al.*, 2004; Huang *et al.*, 2012), which are activated by the PYR/PYL/RCAR-SnRK2-PP2C ABA signaling modules (Danquah *et al.*, 2015). In our study, the MAPK pathway connects drought-induced ABA signaling to the plant immune receptor FLS2 (Supplementary Fig. S8),

which recognizes bacterial flagellin and its immunogenic epitope flg22 to inhibit infection by bacterial pathogens (W.Wang *et al.*, 2020). Interestingly, it was reported that MAPK activation links the late endocytic trafficking of FLS2 specifically with defense-associated stomatal closure (Spallek *et al.*, 2013). We found that the expression of *FLS2* and its recognition receptors (Spallek *et al.*, 2013) was up-regulated in *B. stacei* but down-regulated in *B. hybridum* (Supplementary Fig. S8), suggesting that drought-induced stomatal closure not only affects the expression of genes involved in drought regulation, but also influences other pathways. Our results highlight the significance of the immune-related response in the evolution of *Brachypodium* species genotypes (Fig. 7B; Supplementary Figs S1, S10B), implying that the diploid progenitor *B. stacei* genome may have dominated the response to biotic stresses.

Implications of the adaptations of *B. hybridum* and *B. stacei* in the stress tolerance of grasses

Adaptation is an evolutionary process where traits in a population are naturally selected to better meet environmental challenges (Singaravelan *et al.*, 2008). This study examines the adaptation potential of *Brachypodium* species in the distinct ecological niche of EC. The south-facing AS of EC receives 200–800% higher solar radiation than the temperate north-facing ES, leading to contrasting selective pressures: high light, heat, and drought on the AS, versus shade and pathogens on the ES (Nevo, 2012). Ecological factors shape inter-slope differentiation, with 'water-dependent' groups of organisms being significantly fewer in number on AS than ES (Melamud *et al.*, 2007), while the diversity in the soil microfungal community structure is related to variations in soil moisture and solar radiation (Grishkan and Nevo, 2008). The allotetraploid *B. hybridum* occupies a broader ecological range than its diploid progenitors (López-Alvarez *et al.*, 2015; Catalán *et al.*, 2016): *B. stacei* usually lives in shady habitats, such as the understories of pine forests, juniper woods, and inside spiny shrubs, which protect the plant from direct insolation, whereas *B. hybridum* exhibits greater ecological flexibility, successfully colonizing both mesic and arid environments, predominantly in open, sunny habitats (Catalán *et al.*, 2016). Thus, the two *Brachypodium* species exhibit unique advantages in relation to ecological and environmental adaptation that could guide breeding efforts toward creating climate-resilient cereal crops and pasture grass in the future. In this study, we sampled *B. hybridum* from the dry and high-light AS (the only slope in EC where it is found) (Mu *et al.*, 2023a) and *B. stacei* from the forested and shady ES. This sampling strategy reflects each species' typical habitat preference on the two slopes. It is important to note that *B. stacei* also occurs on the AS, typically sheltered under shrubs (Mu *et al.*, 2023b). Considering that *Brachypodium* species occupy distinct ecological niches (López-Alvarez *et al.*, 2015), one limitation of our study is the absence of *B. distachyon* accessions in EC for comparative analyses. Incorporating a broader range of *B. distachyon* genotypes in future studies would allow a more comprehensive assessment of adaptive strategies across diverse ecological and genetic contexts, thereby strengthening the generalizability of our findings.

Supplementary data

The following supplementary data are available at *JXB* online.

Fig. S1. Top 10 GO terms for ortho-homeolog genes with a ratio of non-synonymous to synonymous substitution rates >1 between *B. hybridum* and *B. stacei*.

Fig. S2. Top 10 GO terms for ortho-homeolog genes with a ratio of non-synonymous to synonymous substitution rates >1 between *B. hybridum* and *B. distachyon*.

Fig. S3. Physiological and stomatal traits of each *Brachypodium* accession collected from the African slope and European slope under well-watered and drought conditions.

Fig. S4. Global transcriptome analysis of the drought response in *B. hybridum* and *B. stacei*.

Fig. S5. Top 10 GO terms for Bhs/Bhd dominant homeologs.

Fig. S6. Homeolog expression bias for each *Brachypodium* accession under the control condition and drought treatment.

Fig. S7. GO and KEGG enrichment analysis of highly connected genes (hub genes) in *B. hybridum* and *B. stacei*.

Fig. S8. Overview of the protein interaction network for WGCNA hub genes in the MAPK pathway of *B. hybridum* and *B. stacei*.

Fig. S9. Protein interaction network for WGCNA hub genes in the MAPK and ABA pathway of *B. hybridum* and *B. stacei*.

Fig. S10. Circos diagram for genome resequencing and long terminal repeat distribution, and GO terms for genes with high-impact SNPs in *B. hybridum* and *B. stacei*.

Table S1. Synteny blocks between Bs and Bh subgenomes.

Table S2. LTR distribution of Bh and Bs genomes.

Table S3. Homeologs under positive selection (Ka/Ks >1) in Bh from both the *stacei*-type and *distachyon*-type subgenomes.

Table S4. Gene expression level of stomatal regulation genes.

Table S5. RNA-seq and resequencing raw reads availability.

Table S6. Homeologs between Bhs and Bhd subgenomes which shifted their dominant subgenome after drought treatment.

Table S7. Annotation for genes with high-impact SNPs in Bh and Bs.

Table S8. Differentially expressed genes in response to drought that were influenced by high-impact SNPs in *B. hybridum* and *B. stacei*.

Acknowledgements

We thank Prof. Kexin Li and Xiaoying Song for providing the seeds.

Author contributions

Z-HC and EN: conceptualization; YW and Z-HC: methodology; YW, GC, and ZY: investigation; YW, GC, and ZH: formal analysis; YW: writing - original draft; PC and Z-HC: writing - review & editing; YW, visualization; FZ and Z-HC: supervision; Z-HC, FD, and SX: funding acquisition.

Conflict of interest

The authors declare that there is no conflict of interest regarding the publication of this manuscript.

Funding

This work was funded by the Australian Research Council (FT210100366), the National Natural Science Foundation of China (31620103912, 31571599, and 31571578). PC was funded by the Spanish Ministry of Science and Innovation TED2021-131073B-I00 and PID2022-140074NB-I00 grants.

Data availability

The data generated in this work are available within the paper and its supplementary data. The raw reads for the RNA sequences and whole-genome sequencing were obtained from published datasets; these datasets are available from NCBI BioProjects (PRJNA628850) and (PRJNA688592).

References

Abdoli M, Moieni A, Naghdi Badi H. 2013. Morphological, physiological, cytological and phytochemical studies in diploid and colchicine-induced tetraploid plants of *Echinacea purpurea* (L.). Acta Physiologiae Plantarum **35**, 2075–2083.

Adamczyk BJ, Fernandez DE. 2009. MIKC* MADS domain heterodimers are required for pollen maturation and tube growth in Arabidopsis. Plant Physiology **149**, 1713–1723.

Adem GD, Chen G, Shabala L, Chen Z-H, Shabala S. 2020. GORK channel: a master switch of plant metabolism? Trends in Plant Science **25**, 434–445.

Bai X, Shen W, Wu X, Wang P. 2020. Applicability of long-term satellite-based precipitation products for drought indices considering global warming. Journal of Environmental Management **255**, 109846.

Baidouri ME, Panaud O. 2013. Comparative genomic paleontology across plant kingdom reveals the dynamics of TE-driven genome evolution. Genome Biology and Evolution **5**, 954–965.

Borrino EM, Powell W. 1988. Stomatal guard cell length as an indicator of ploidy in microspore-derived plants of barley. Genome **30**, 158–160.

Brkljacic J, Grotewold E, Scholl R, *et al*. 2011. Brachypodium as a model for the grasses: today and the future. Plant Physiology **157**, 3–13.

Bromham L, Hua X, Cardillo M. 2020. Macroevolutionary and macroecological approaches to understanding the evolution of stress tolerance in plants. Plant, Cell & Environment **43**, 2832–2846.

Brutnell TP, Bennetzen JL, Vogel JP. 2015. *Brachypodium distachyon* and *Setaria viridis*: model genetic systems for the grasses. Annual Review of Plant Biology **66**, 465–485.

Cai S, Huang Y, Chen F, *et al*. 2021. Evolution of rapid blue-light response linked to explosive diversification of ferns in angiosperm forests. New Phytologist **230**, 1201–1213.

Caperta AD, Róis AS, Teixeira G, Garcia-Caparros P, Flowers TJ. 2020. Secretory structures in plants: lessons from the Plumbaginaceae on their origin, evolution and roles in stress tolerance. Plant Cell and Environment **43**, 2912–2931.

Carruthers T, Gonçalves DJP, Li P, *et al*. 2024. Repeated shifts out of tropical climates preceded by whole genome duplication. New Phytologist **244**, 2561–2575.

Catalán P, López-Álvarez D, Bellosta C, Villar L. 2016. Updated taxonomic descriptions, iconography, and habitat preferences of *Brachypodium distachyon*, *B. stacei*, and *B. hybridum* (Poaceae). Anales del Jardin Botanico de Madrid **73**, e028.

Catalán P, Müller J, Hasterok R, Jenkins G, Mur LAJ, Langdon T, Betekhtin A, Siwinska D, Pimentel M, López-Alvarez D. 2012. Evolution and taxonomic split of the model grass *Brachypodium distachyon*. Annals of Botany **109**, 385–405.

Chao DY, Dilkes B, Luo H, Douglas A, Yakubova E, Lahner B, Salt DE. 2013. Polyploids exhibit higher potassium uptake and salinity tolerance in *Arabidopsis*. Science **341**, 658–659.

Chaves MM, Maroco JP, Pereira JS. 2003. Understanding plant responses to drought — from genes to the whole plant. Functional Plant Biology **30**, 239–264.

Chen G, Wang Y, Wang X, *et al*. 2019. Leaf epidermis transcriptome reveals drought-induced hormonal signaling for stomatal regulation in wild barley. Plant Growth Regulation **87**, 39–54.

Chen X, Cheng J, Chen L, Zhang G, Huang H, Zhang Y, Xu L. 2016. Auxin-independent *NAC* pathway acts in response to explant-specific wounding and promotes root tip emergence during de novo root organogenesis in Arabidopsis. Plant Physiology **170**, 2136–2145.

Chinnusamy V, Schumaker K, Zhu JK. 2004. Molecular genetic perspectives on cross-talk and specificity in abiotic stress signalling in plants. Journal of Experimental Botany **55**, 225–236.

Danquah A, De Zélicourt A, Boudsocq M, *et al*. 2015. Identification and characterization of an ABA-activated MAP kinase cascade in *Arabidopsis thaliana*. The Plant Journal **82**, 232–244.

Deng B, Du W, Liu C, Sun W, Tian S, Dong H. 2012. Antioxidant response to drought, cold and nutrient stress in two ploidy levels of tobacco plants: low resource requirement confers polytolerance in polyploids? Plant Growth Regulation **66**, 37–47.

Dittberner H, Korte A, Mettler-Altmann T, Weber APM, Monroe G, de Meaux J. 2018. Natural variation in stomata size contributes to the local adaptation of water-use efficiency in A*rabidopsis thaliana*. Molecular Ecology **27**, 4052–4065.

Dong Y, Hu G, Grover CE, Miller ER, Zhu S, Wendel JF. 2022. Parental legacy versus regulatory innovation in salt stress responsiveness of allopolyploid cotton (*Gossypium*) species. The Plant Journal **111**, 872–887.

Donovan LA, Dudley SA, Rosenthal DM, Ludwig F. 2007. Phenotypic selection on leaf water use efficiency and related ecophysiological traits for natural populations of desert sunflowers. Oecologia **152**, 13–25.

Doyle JJ, Coate JE. 2019. Polyploidy, the nucleotype, and novelty: the impact of genome doubling on the biology of the cell. International Journal of Plant Sciences **180**, 1–52.

Draper J, Mur LAJ, Jenkins G, Ghosh-Biswas GC, Bablak P, Hasterok R, Routledge APM. 2001. *Brachypodium distachyon*. A new model system for functional genomics in grasses. Plant Physiology **127**, 1539–1555.

Du H, Huang F, Wu N, Li X, Hu H, Xiong L. 2018. Integrative regulation of drought escape through ABA-dependent and -independent pathways in rice. Molecular Plant **11**, 584–597.

Ebadi M, Bafort Q, Mizrachi E, Audenaert P, Simoens P, Van Montagu M, Bonte D, Van de Peer Y. 2023. The duplication of genomes and genetic networks and its potential for evolutionary adaptation and survival during environmental turmoil. Proceedings of the National Academy of Sciences, USA **120**, e2307289120.

Fawcett JA, Maere S, Van De Peer Y. 2009. Plants with double genomes might have had a better chance to survive the Cretaceous–Tertiary

extinction event. Proceedings of the National Academy of Sciences, USA **106**, 5737–5742.

Feldman M, Levy AA, Fahima T, Korol A. 2012. Genomic asymmetry in allopolyploid plants: wheat as a model. Journal of Experimental Botany **63**, 5045–5059.

Frawley LE, Orr-Weaver TL. 2015. Polyploidy. Current Biology **25**, R353–R358.

Godfray HCJ, Beddington JR, Crute IR, Haddad L, Lawrence D, Muir JF, Pretty J, Robinson S, Thomas SM, Toulmin C. 2010. Food security: the challenge of feeding 9 billion people. Science **327**, 812–818.

Godfray HCJ, Pretty J, Thomas SM, Warham EJ, Beddington JR. 2011. Linking policy on climate and food. Science **331**, 1013–1014.

González JM, Redondo-Pedraza J, Loarce Y, Hammami R, Friero E, Jouve N. 2020. Molecular genetic analysis of drought stress response traits in *Brachypodium* spp. Agronomy **10**, 518.

Gordon SP, Contreras-Moreira B, Levy JJ, *et al*. 2020. Gradual polyploid genome evolution revealed by pan-genomic analysis of *Brachypodium hybridum* and its diploid progenitors. Nature Communications **11**, 3670.

Grishkan I, Nevo E. 2008. Vertical divergence of microfungal communities in soil profiles of 'Evolution Canyon' I, Lower Nahal Oren, Mount Carmel, Israel. Plant Biosystems **142**, 51–59.

Grundy J, Stoker C, Carré IA. 2015. Circadian regulation of abiotic stress tolerance in plants. Frontiers in Plant Science **6**, 648.

Gui Y, Sheteiwy MS, Zhu S, Zhu L, Batool A, Jia T, Xiong Y. 2021. Differentiate responses of tetraploid and hexaploid wheat (*Triticum aestivum* L.) to moderate and severe drought stress: a cue of wheat domestication. Plant Signaling & Behavior **16**, 1839710.

He N, Zhang C, Qi X, *et al*. 2013. Draft genome sequence of the mulberry tree *Morus notabilis*. Nature Communications **4**, 2445.

Henry C, John GP, Pan R, Bartlett MK, Fletcher LR, Scoffoni C, Sack L. 2019. A stomatal safety-efficiency trade-off constrains responses to leaf dehydration. Nature Communications **10**, 3398.

Heschel MS, Riginos C. 2005. Mechanisms of selection for drought stress tolerance and avoidance in *Impatiens capensis* (Balsaminaceae). American Journal of Botany **92**, 37–44.

Heslop-Harrison JS, Schwarzacher T, Liu Q. 2023. Polyploidy: its consequences and enabling role in plant diversification and evolution. Annals of Botany **131**, 1–10.

Huang GT, Ma SL, Bai LP, Zhang L, Ma H, Jia P, Liu J, Zhong M, Guo ZF. 2012. Signal transduction during cold, salt, and drought stresses in plants. Molecular Biology Reports **39**, 969–987.

Ivey CT, Carr DE. 2012. Tests for the joint evolution of mating system and drought escape in *Mimulus*. Annals of Botany **109**, 583–598.

Kang L, Rashkovetsky E, Michalak K, Garner HR, Mahaney JE, Rzigalinski BA, Korol A, Nevo E, Michalak P. 2019. Genomic divergence and adaptive convergence in *Drosophila simulans* from Evolution Canyon, Israel. Proceedings of the National Academy of Sciences, USA **116**, 11839–11844.

Katsiotis A, Forsberg RA. 1995. Pollen grain size in four ploidy levels of genus *Avena*. Euphytica **83**, 103–108.

Khalid MF, Huda S, Yong M, Li LH, Li L, Chen ZH, Ahmed T. 2023. Alleviation of drought and salt stress in vegetables: crop responses and mitigation strategies. Plant Growth Regulation **99**, 177–194.

Kondrashov FA. 2012. Gene duplication as a mechanism of genomic adaptation to a changing environment. Proceedings: Biological Sciences **279**, 5048–5057.

Kurtz LE, Brand MH, Lubell-Brand JD. 2020. Production of tetraploid and triploid hemp. HortScience **55**, 1703–1707.

Landis JB, Soltis DE, Li Z, Marx HE, Barker MS, Tank DC, Soltis PS. 2018. Impact of whole-genome duplication events on diversification rates in angiosperms. American Journal of Botany **105**, 348–363.

Langfelder P, Zhang B, Horvath S. 2008. Defining clusters from a hierarchical cluster tree: the dynamic tree cut package for R. Bioinformatics **24**, 719–720.

Lesk C, Rowhani P, Ramankutty N. 2016. Influence of extreme weather disasters on global crop production. Nature **529**, 84–87.

Li K, Wang H, Cai Z, Wang L, Xu Q, Lövy M, Wang Z, Nevo E. 2016. Sympatric speciation of spiny mice, *Acomys*, unfolded transcriptomically at Evolution Canyon, Israel. Proceedings of the National Academy of Sciences, USA **113**, 8254–8259.

Liu C, Ren Y, Li Z, *et al*. 2020. Giant African snail genomes provide insights into molluscan whole-genome duplication and aquatic–terrestrial transition. Molecular Ecology Resources **21**, 478–494.

Liu X, Fan Y, Mak M, *et al*. 2017. QTLs for stomatal and photosynthetic traits related to salinity tolerance in barley. BMC Genomics **18**, 9.

López-Alvarez D, Manzaneda AJ, Rey PJ, *et al*. 2015. Environmental niche variation and evolutionary diversification of the *Brachypodium distachyon* grass complex species in their native circum-Mediterranean range. American Journal of Botany **102**, 1073–1088.

López-Álvarez D, Zubair H, Beckmann M, Draper J, Catalán P. 2017. Diversity and association of phenotypic and metabolomic traits in the close model grasses *Brachypodium distachyon*, *B. stacei* and *B. hybridum*. Annals of Botany **119**, 545–561.

Love MI, Huber W, Anders S. 2014. Moderated estimation of fold change and dispersion for RNA-seq data with DESeq2. Genome Biology **15**, 1–21.

Lynch M, Conery JS. 2000. The evolutionary fate and consequences of duplicate genes. Science **290**, 1151–1155.

Ma H, Lin J, Mei F, Mao H, Li QQ. 2023. Differential alternative polyadenylation of homoeologous genes of allohexaploid wheat ABD subgenomes during drought stress response. The Plant Journal **114**, 499–518.

Mahmoud LM, Killiny N, Holden P, Gmitter FG Jr, Grosser JW, Dutt M. 2023. Physiological and biochemical evaluation of salt stress tolerance in a citrus tetraploid somatic hybrid. Horticulturae **9**, 1215.

Makova KD, Li WH. 2003. Divergence in the spatial pattern of gene expression between human duplicate genes. Genome Research **13**, 1638–1645.

Manzaneda AJ, Rey PJ, Anderson JT, Raskin E, Weiss-Lehman C, Mitchell-Olds T. 2015. Natural variation, differentiation, and genetic trade-offs of ecophysiological traits in response to water limitation in *Brachypodium distachyon* and its descendent allotetraploid *B. hybridum* (Poaceae). Evolution **69**, 2689–2704.

Manzaneda AJ, Rey PJ, Bastida JM, Weiss-Lehman C, Raskin E, Mitchell-Olds T. 2012. Environmental aridity is associated with cytotype segregation and polyploidy occurrence in *Brachypodium distachyon* (Poaceae). New Phytologist **193**, 797–805.

Masterson J. 1994. Stomatal size in fossil plants: evidence for polyploidy in majority of angiosperms. Science **264**, 421–424.

Mattingly KZ, Hovick SM. 2023. Autopolyploids of *Arabidopsis thaliana* are more phenotypically plastic than their diploid progenitors. Annals of Botany **131**, 45–58.

McKay JK, Richards JH, Mitchell-Olds T. 2003. Genetics of drought adaptation in *Arabidopsis thaliana*: I. Pleiotropy contributes to genetic correlations among ecological traits. Molecular Ecology **12**, 1137–1151.

Melamud V, Beharav A, Pavlíček T, Nevo E. 2007. Biodiversity interslope divergence of oribatid mites at 'evolution canyon', Mount Carmel, Israel. Acta Zoologica Academiae Scientiarum Hungaricae **53**, 381–396.

Mu W, Li K, Yang Y, *et al*. 2023a. Subgenomic stability of progenitor genomes during repeated allotetraploid origins of the same grass *Brachypodium hybridum*. Molecular Biology and Evolution **40**, msad259.

Mu W, Li K, Yang Y, *et al*. 2023b. Scattered differentiation of unlinked loci across the genome underlines ecological divergence of the selfing grass *Brachypodium stacei*. Proceedings of the National Academy of Sciences, USA **120**, e2304848120.

Murat F, Xu JH, Tannier E, Abrouk M, Guilhot N, Pont C, Messing J, Salse J. 2010. Ancestral grass karyotype reconstruction unravels new mechanisms of genome shuffling as a source of plant evolution. Genome Research **20**, 1545–1557.

Nelson CW, Moncla LH, Hughes AL. 2015. SNPGenie: estimating evolutionary parameters to detect natural selection using pooled next-generation sequencing data. Bioinformatics **31**, 3709–3711.

Nevo E. 1995. Asian, African and European biota meet at 'Evolution Canyon' Israel: local tests of global biodiversity and genetic diversity patterns. Proceedings: Biological Sciences **262**, 149–155.

Nevo E. 2012. 'Evolution Canyon', a potential microscale monitor of global warming across life. Proceedings of the National Academy of Sciences, USA **109**, 2960–2965.

Oliver KR, McComb JA, Greene WK. 2013. Transposable elements: powerful contributors to angiosperm evolution and diversity. Genome Biology and Evolution **5**, 1886–1901.

Ou S, Jiang N. 2018. LTR_retriever: a highly accurate and sensitive program for identification of long terminal repeat retrotransposons. Plant Physiology **176**, 1410–1422.

Parsons JL, Martin SL, James T, Golenia G, Boudko EA, Hepworth SR. 2019. Polyploidization for the genetic improvement of *Cannabis sativa*. Frontiers in Plant Science **10**, 476–p.449166.

Ramírez-González RH, Borrill P, Lang D, *et al*. 2018. The transcriptional landscape of polyploid wheat. Science **361**, eaar6089.

Ramsey J, Schemske DW. 1998. Pathways, mechanisms, and rates of polyploid formation in flowering plants. Annual Reviews of Ecology and Systematics **29**, 467–501.

Renny-Byfield S, Wendel JF. 2014. Doubling down on genomes: polyploidy and crop plants. American Journal of Botany **101**, 1711–1725.

Ruiz M, Quiñones A, Martínez-Cuenca MR, Aleza P, Morillon R, Navarro L, Primo-Millo E, Martínez-Alcántara B. 2016. Tetraploidy enhances the ability to exclude chloride from leaves in carrizo citrange seedlings. Journal of Plant Physiology **205**, 1–10.

Sancho R, Cantalapiedra CP, López-Alvarez D, Gordon SP, Vogel JP, Catalán P, Contreras-Moreira B. 2018. Comparative plastome genomics and phylogenomics of *Brachypodium*: flowering time signatures, introgression and recombination in recently diverged ecotypes. New Phytologist **218**, 1631–1644.

Sherrard ME, Maherali H. 2006. The adaptive significance of drought escape in *Avena barbata*, an annual grass. Evolution **60**, 2478–2489.

Shimizu-Inatsugi R, Terada A, Hirose K, Kudoh H, Sese J, Shimizu KK. 2017. Plant adaptive radiation mediated by polyploid plasticity in transcriptomes. Molecular Ecology **26**, 193–207.

Singaravelan N, Grishkan I, Beharav A, Wakamatsu K, Ito S, Nevo E. 2008. Adaptive melanin response of the soil fungus *Aspergillus niger* to UV radiation stress at 'Evolution Canyon', Mount Carmel, Israel. PLoS One **3**, e2993.

Šmarda P, Klem K, Knápek O, Veselá B, Veselá K, Holub P, Kuchař V, Šilerová A, Horová L, Bureš P. 2023. Growth, physiology, and stomatal parameters of plant polyploids grown under ice age, present-day, and future CO_2 concentrations. New Phytologist **239**, 399–414.

Soltis DE, Visger CJ, Soltis PS. 2014. The polyploidy revolution then... and now: Stebbins revisited. American Journal of Botany **101**, 1057–1078.

Spallek T, Beck M, Ben Khaled S, Salomon S, Bourdais G, Schellmann S, Robatzek S. 2013. ESCRT-I mediates FLS2 endosomal sorting and plant immunity. PLoS Genetics **9**, e1004035.

Srivastava D, Shamim M, Kumar M, Mishra A, Maurya R, Sharma D, Pandey P, Singh KN. 2019. Role of circadian rhythm in plant system: an update from development to stress response. Environmental and Experimental Botany **162**, 256–271.

Su G, Morris JH, Demchak B, Bader GD. 2014. Biological network exploration with cytoscape 3. Current Protocols in Bioinformatics **47**, 8.13.1–18.13.24.

Takahagi K, Inoue K, Shimizu M, Uehara-Yamaguchi Y, Onda Y, Mochida K. 2018. Homoeolog-specific activation of genes for heat acclimation in the allopolyploid grass *Brachypodium hybridum*. GigaScience **7**, giy020.

The International Brachypodium Initiative. 2010. Genome sequencing and analysis of the model grass *Brachypodium distachyon*. Nature **463**, 763–768.

Tuberosa R. 2012. Phenotyping for drought tolerance of crops in the genomics era. Frontiers in Physiology **3**, 347.

Van de Peer Y, Ashman T-L, Soltis PS, Soltis DE. 2020. Polyploidy: an evolutionary and ecological force in stressful times. The Plant Cell **33**, 11–26.

Van de Peer Y, Mizrachi E, Marchal K. 2017. The evolutionary significance of polyploidy. Nature Reviews. Genetics **18**, 411–424.

van Laere K, França SC, Vansteenkiste H, van Huylenbroeck J, Steppe K, van Labeke MC. 2011. Influence of ploidy level on morphology, growth and drought susceptibility in *Spathiphyllum wallisii*. Acta Physiologiae Plantarum **33**, 1149–1156.

Wang H, Yin H, Jiao C, *et al*. 2020. Sympatric speciation of wild emmer wheat driven by ecology and chromosomal rearrangements. Proceedings of the National Academy of Sciences, USA **117**, 5955–5963.

Wang N-H, Zhou X-Y, Shi S-H, Zhang S, Chen Z-H, Ali MA, Ahmed IM, Wang Y, Wu F. 2023. An miR156-regulated nucleobase-ascorbate transporter 2 confers cadmium tolerance via enhanced anti-oxidative capacity in barley. Journal of Advanced Research **44**, 23–37.

Wang W, Liu N, Gao C, Cai H, Romeis T, Tang D. 2020. The Arabidopsis exocyst subunits EXO70B1 and EXO70B2 regulate FLS2 homeostasis at the plasma membrane. New Phytologist **227**, 529–544.

Wang Y, Chen G, Zeng F, *et al*. 2023. Molecular evidence for adaptive evolution of drought tolerance in wild cereals. New Phytologist **237**, 497–514.

Wang Y, Chen ZH. 2020. Does molecular and structural evolution shape the speedy grass stomata? Frontiers in Plant Science **11**, 333.

Wang Y, Tang H, Debarry JD, *et al*. 2012. *MCScanX*: a toolkit for detection and evolutionary analysis of gene synteny and collinearity. Nucleic Acids Research **40**, e49.

Wicker T, Buchmann JP, Keller B. 2010. Patching gaps in plant genomes results in gene movement and erosion of colinearity. Genome Research **20**, 1229–1237.

Wu CA, Lowry DB, Nutter LI, Willis JH. 2010. Natural variation for drought-response traits in the *Mimulus guttatus* species complex. Oecologia **162**, 23–33.

Xing SH, Guo XB, Wang Q, Pan QF, Tian YS, Liu P, Zhao JY, Wang GF, Sun XF, Tang KX. 2011. Induction and flow cytometry identification of tetraploids from seed-derived explants through colchicine treatments in *Catharanthus roseus* (L.) G. Don. Biomed Research International **2011**, 793198.

Xiong L, Yang Y. 2003. Disease resistance and abiotic stress tolerance in rice are inversely modulated by an abscisic acid-inducible mitogen-activated protein kinase. The Plant Cell **15**, 745–759.

Yablonovitch AL, Fu J, Li K, *et al*. 2017. Regulation of gene expression and RNA editing in *Drosophila* adapting to divergent microclimates. Nature Communications **8**, 1570.

Yang C, Zhao L, Zhang H, Yang Z, Wang H, Wen S, Zhang C, Rustgi S, Von Wettstein D, Liu B. 2014. Evolution of physiological responses to salt stress in hexaploid wheat. Proceedings of the National Academy of Sciences, USA **111**, 11882–11887.

Yang PM, Huang QC, Qin GY, Zhao SP, Zhou JG. 2014. Different drought-stress responses in photosynthesis and reactive oxygen metabolism between autotetraploid and diploid rice. Photosynthetica **52**, 193–202.

Zhang L, Wu S, Chang X, Wang X, Zhao Y, Xia Y, Trigiano RN, Jiao Y, Chen F. 2020. The ancient wave of polyploidization events in flowering plants and their facilitated adaptation to environmental stress. Plant, Cell & Environment **43**, 2847–2856.

Zhu H, Zhao S, Lu X, He N, Gao L, Dou J, Bie Z, Liu W. 2018. Genome duplication improves the resistance of watermelon root to salt stress. Plant Physiology and Biochemistry **133**, 11–21.

Zwaenepoel A, Van De Peer Y. 2019. wgd—simple command line tools for the analysis of ancient whole-genome duplications. Bioinformatics **35**, 2153–2155.